Journal of Physics: Conference Series **549** (2014) 012022 doi:10.1088/1742-6596/549/1/012022

Neutron structural characterization and transport properties of the oxidized and reduced $LaCo_{0.5}Ti_{0.5}O_3$ perovskite oxide.

R. Martinez-Coronado[1], A. Aguadero[2], J.A. Alonso[1], D. Perez-Coll[3], M.T. Fernandez-Díaz[4].

[1]Instituto de Ciencia de Materiales de Madrid, C.S.I.C., Cantoblanco E-28049 Madrid.
[2]CIC Energigune, Albert Einstein 48, 01510 Alava, Spain
[3]Instituto de Cerámica y Vidrio-CSIC, Cantoblanco, 28049 Madrid, Spain
[4]Institut Laue Langevin, BP 156X, Grenoble, F-38042, France

E-mail: rmartinez@icmm.csic.es

Abstract. Polycrystalline oxygen-stoichiometric $LaCo_{0.5}Ti_{0.5}O_3$ perovskite oxide has been prepared by soft-chemistry procedures followed by annealing in air at 800ºC. A new reduced $LaCo_{0.5}Ti_{0.5}O_{3-\delta}$ specimen has been obtained by topotactical oxygen removal in an H_2/N_2 (5%/95%) flow at 600ºC. The structural characterization has been conducted from neutron powder diffraction (NPD) data, very sensitive to the contrast between Co and Ti and the oxygen stoichiometry. Both perovskites (oxidized and reduced) crystallize in the orthorhombic *Pbnm,* space group. The partial reduction of Ti^{4+} to Ti^{3+} in the reduced phase is accompanied with the occurrence of oxygen vacancies, located at the axial octahedral sites, and it is expected to support the ionic conductivity, as usually observed in oxygen-defective perovskites. Thermogravimetric analysis (TGA) substantiates the oxygen stoichiometry and the stability range of the reduced sample. All the samples in study display a semiconductor-like behavior with values that not reach below to 0.5 Scm^{-1} for all the phases. Moreover, the measured thermal expansion coefficients perfectly match with the values usually displayed by SOFC electrolytes.

1. Introduction

Materials with perovskite-like structure are receiving great attention due to their vast range of possible applications. Perovskite-type oxides are widely used as functional materials in ferroelectric, thermoelectric, dielectric, magnetoelectronic devices and in solid oxide fuel cells (SOFC), among wide panoply of applications. Their unique properties derive from an unmatched chemical flexibility in spite of their relatively simple crystal structure [1]. The reduction of stoichiometric phases into novel oxygen hypo-stoichiometric oxides is a powerful tool for the development of new materials with novel magnetic or transport properties [2]. Moreover, the stabilization of transition-metal perovskites with an adequate concentration of oxygen vacancies under reducing atmosphere can also be of application in new mixed electronic-ionic conductors for energy-conversion devices such as solid oxide fuel cells, oxygen separation membranes or solid oxide electrolyzers.

Owing to many interesting properties such as rich structural characteristics, transport and magnetic properties [3-6], perovskites oxides of $R(III)Ti(III)O_3$ (R= rare earth) have been one of the hot subjects of recent studies. Among perovskite oxides that exhibit appealing properties, ceramic titanates are recognized to present high stability under reducing environments with high tolerance to sulphur poisoning. The formation of $R(M,Ti)O_3$ (R= rare earth; M= metal transition) is may be feasible either for trivalent M and Ti ions (having in mind that Ti^{3+} ions are difficult to stabilize) or with a combination of divalent M and tetravalent Ti ionic states, under the appropriate atmosphere during the high-temperature synthesis [7]. When Co(III) ions are substituted by Ti(IV), as reported in the $LaCo_{1-x}Ti_xO_3$ solid solution [8], a mixed valence system is obtained as the charge neutrality requires the partial reduction to divalent Co ions.

$LaCo_{0.5}Ti_{0.5}O_3$ perovskite has been previously reported by several researchers, which defined the crystal structure by neutron powder diffraction in both orthorhombic and monoclinic unit-cell [9-11]; also x-ray diffraction, thermogravimetric analysis and magnetic susceptibilities were used to characterize this material [12]. Although there is a comprehensive study of this perovskite, the research of the reducibility has not been yet considered.

In this work we have analyzed the reducibility of the $LaCo_{0.5}Ti_{0.5}O_3$ perovskite and the crystal structure evolution from the oxidized to the reduced phase. The analysis of NPD data for both oxidized and reduced specimens suggests the presence of Ti^{3+}-Ti^{4+} mixed valence in the reduced phase. The characterization has been completed with thermal expansion, electric conductivity measurements and thermal analysis under oxidizing and reducing atmosphere.

2. Experimental

$LaCo_{0.5}Ti_{0.5}O_3$ perovskite was prepared as a polycrystalline powder from citrate precursors obtained by soft-chemistry procedures. Stoichiometric amounts La_2O_3 (pre-dried at 900ºC), $Co(NO_3)_2{\cdot}6H_2O$ and $TiC_{10}H_{14}O_5$ were solved in citric acid and some drops of nitric acid. The solution was then slowly evaporated, in order to favor the dissolution of the rare-earth oxide, leading to organic resins that contain a homogeneous distribution of the involved cations. The formed resins were dried at 120 ºC and decomposed at 600 ºC for 12 h, heating with a 50 $ºC{\cdot}h^{-1}$ ramp, in air. All the organic materials and nitrates were eliminated in a subsequent treatment at 800°C in air, for 2 hours, which gave rise to the pure perovskite oxide phase. The reduced $LaCo_{0.5}Ti_{0.5}O_{3-\delta}$ perovskites were prepared by treating the oxidized phase under an $5\%H_2/95\%N_2$ flow (60 mL min^{-1}) at 600 ºC for 4 h in alumina boats.

The initial characterization of the product was carried out by XRD with a Bruker-axs D8 Advanced diffractometer (40 kV, 30 mA), controlled by a DIFFRACT^{PLUS} software, in Bragg-Brentano reflection geometry with Cu K_α radiation (λ = 1.5418 Å) and a PSD (Position Sensitive Detector). A filter of nickel allows the complete removal of Cu K_β radiation. For the structural refinement NPD patterns were collected at the D1A diffractometer of the ILL, Grenoble, with a wavelength λ= 1.910 Å at room temperature. About 2 g of the sample were contained in a vanadium can and placed in the isothermal zone of a furnace with a vanadium resistor operating under vacuum ($P_{O2} \approx 10^{-6}$ Torr), and the counting time was 2 h per pattern in the high-intensity mode. The NPD data were analyzed by the Rietveld method [13] with the FULLPROF program [14]. A pseudo-Voigt function was chosen to generate the line shape of the diffraction peaks. The following parameters were refined in the final run: scale factor, background coefficients, zero-point error, pseudo-Voigt corrected for asymmetry parameters, positional coordinates and isotropic thermal factors for all the atoms. The coherent scattering lengths for La, Co, Ti and O were 8.24, 2.49, -3.438 and 5.803 fm, respectively [14].

Thermal analysis was carried out in a Mettler TA3000 system equipped with a TC10 processor unit. Thermogravimetric (TG) curves were obtained in a TG50 unit, working at a heating rate of 10 °C min^{-1}, in a reducing $H_2(5\%)/N_2(95\%)$ flow of 0.3 L min^{-1}. The heating rate was 10 °C min^{-1}, using about 50 mg of sample in each experiment.

Measurements of the thermal expansion coefficient and electrical conductivity required the use of sintered samples. The obtained density is around 90-95%. Thermal expansion of the sintered samples was performed in a dilatometer Linseis L75HX1000, between 300 and 800 ºC in air and

H_2(5%)/N_2(95%) atmospheres. The conductivity was measured between 25 and 850 ºC in the requested atmosphere, by the four-point method in bar-shaped pellets under DC currents between 0.05 and 0.10 A. The currents were applied and collected with a Potenciostat-Galvanostat AUTOLAB PGSTAT 302 from ECO CHEMIE.

3. Results and Discussion

3.1. Crystal structure

The oxidized and reduced $LaCo_{0.5}Ti_{0.5}O_3$ perovskites were obtained as well-crystallized powders. Single-orthorhombic perovskite phases were identified from laboratory XRD (Fig. 1) for the reduced and oxidized sample. No impurity phases were detected.

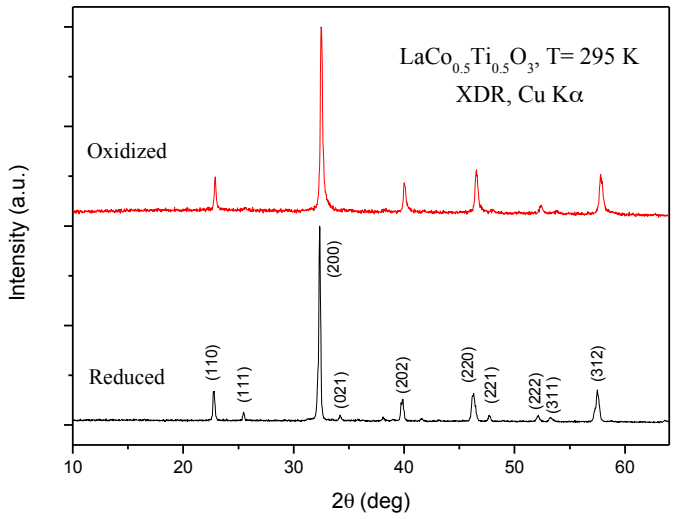

Fig. 1. (Color online) XRD patterns with Cu Kα radiation for $LaCo_{0.5}Ti_{0.5}O_3$, characteristic of pure orthorhombic perovskite phases.

To carry out a more accurate structural study of the $LaM_{0.5}Ti_{0.5}O_3$ (M= Co and Ni) oxides, we performed a NPD investigation at room temperature for all the perovskites; neutrons are especially sensitive to the nature of these atoms since they show very contrasting (positive for Co and negative for Ti) scattering lengths. The crystal structure of the oxidized and reduced $LaCo_{0.5}Ti_{0.5}O_3$ is defined in the orthorhombic *Pbnm* space group (No. 62), Z=4, as was previously reported by Clairns et al. [11]. La and O1 atoms are located at 4*c* (x,y,1/4) positions, M and Ti distributed at random at 4*b* (1/2,0,0), and oxygen atoms O2 at 8*d* (x,y,z). Therefore, for both oxidized and reduced phases the Co and Ti atoms are randomly distributed and no crystallographic long-range order was observed.

The refinement of the occupancy factors of the oxygen atoms for the oxidized phase led to a full stoichiometry, while the reduced phase shows oxygen vacancies concomitant with the presence of Ti^{3+}. The vacancies are concentrated at O1 sites (axial oxygen atoms); O2 showed occupancies slightly higher than 1 and was then fixed to unity. The refined occupancy factors of oxygen atoms for the reduced phase lead to the $LaCo_{0.5}Ti_{0.5}O_{2.91(1)}$ stoichiometry. Fig. 2 illustrates the good agreement between the observed and calculated NPD patterns for the oxidized and reduced $LaCo_{0.5}Ti_{0.5}O_3$ at room temperature.

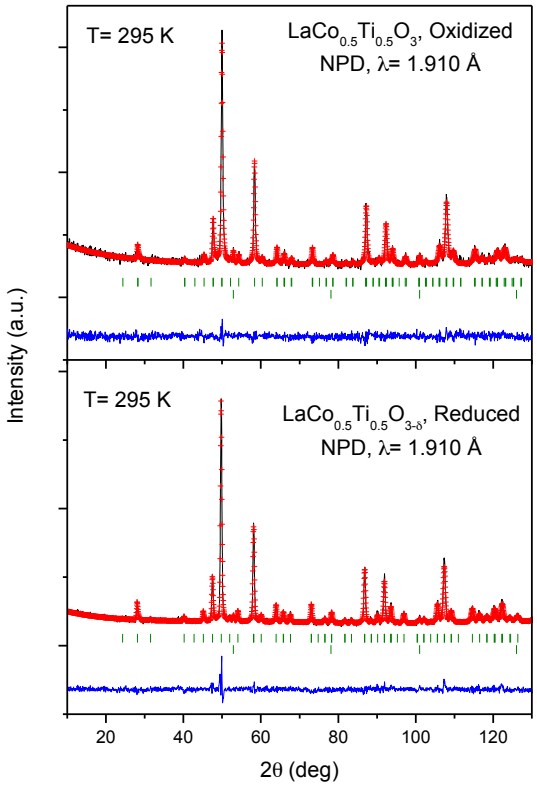

Fig. 2. (Color online) Observed (crosses), calculated (full line) and difference (at the bottom) NPD profiles for reduced and oxidized $LaCo_{0.5}Ti_{0.5}O_3$ at 295 K, refined in the orthorhombic *Pbnm* space group. The two series of tick marks correspond to the positions of the allowed Bragg reflections for the main phase and vanadium.

An alternative refinement of the crystal structure of the oxidized and reduced samples was carried out in the monoclinic $P2_1/n$ space group; in this model the Rietveld refinements display the existence of a certain level of anti-site disorder between Co and Ti cations. However, the results of the refinement at $P2_1/n$ are similar to those obtained with the *Pbnm*; the R_{Bragg} discrepancy factor is practically the same (10%) and the displacement B factors for Zn and Mn become unrealistically high (around 5 $Å^2$); therefore this model was discarded. This is in disagreement with the results by Rodriguez [10], who described an monoclinic $P2_1/n$ symmetry for the $La(Co,Ti)O_3$ from NPD data.

Previous reports of the $LaCo_{0.5}Ti_{0.5}O_3$ perovskite have achieved similar R_{Bragg} discrepancy factor for the disordered model in *Pnma* and the ordered model in $P2_1/n$ [10,11]. Refinements in the ordered model revealed small amounts of intermixing (5%) of Co and Ti on the B and B′ sites. The refinements show that the higher-temperature synthesis (1300 °C) method gives more complete B site ordering than was found for the lower-temperature synthesis is temperature (900 °C) method previously reported [10].

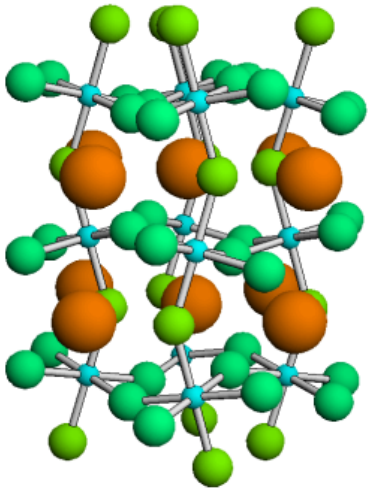

Fig. 3. Schematic view of the orthorhombic crystal structure of $LaCo_{0.5}Ti_{0.5}O_3$.

Fig. 3 sketch the crystal structure observed in both the oxidized and reduced phases, which is defined in the orthorhombic *Pbnm* ($a^-a^-c^+$) space group. Table I summarizes the unit-cell, atomic, thermal parameters and discrepancy factors after the Rietveld refinements of all the samples at room temperature. The cell volume of the reduced phase (242.92(1) $Å^3$) are expanded with respect to the oxidized sample (240.29(1) $Å^3$), as expected from the larger size of Ti^{3+} (i.r.: 0.650 Å) *vs* Ti^{4+} (i.r.: 0.605 Å) [15].

Table I. Unit-cell and thermal parameters for the oxidized and reduced $LaM_{0.5}Ti_{0.5}O_3$ (M= Co and Ni) in orthorhombic *Pbnm* (No. 62) space group, from NPD at 295K. La and O1 at 4*c* (x,y,1/4) positions, Co/Ti at 4*b* (1/2,0,0), and O2 at 8*d* (x,y,z).

M	**Co (oxidized)**	**Co (reduced)**
a (Å)	5.5457(2)	5.5605(1)
b (Å)	5.5344(2)	5.5608(2)
c (Å)	7.8292(2)	7.8562(1)
V ($Å^3$)	240.29(1)	242.92(1)
La 4c (x,y,1/4)		
x	1.0011(3)	0.9996(3)
y	0.0249(2)	0.0246(1)
B_{iso}	1.1(2)	1.5(2)
f_{occ}	1.00	1.00
Ti/M 4b (1/2,0,0)		
B_{iso}	0.30	0.30
Ti/M f_{occ}	0.50/0.50	0.50/0.50
O1 4c (x,y,1/4)		
x	0.0678(4)	0.0661(3)
y	0.4992(3)	0.4906(2)
B_{iso}	1.4(4)	0.9(2)
f_{occ}	1.00	0.91(2)
O2 8d (x,y,z)		
x	0.7163(2)	0.7182(2)

y	0.2717(3)	0.2826(2)
z	0.0376(2)	0.0404(1)
B_{iso}	1.2(2)	1.4(2)
f_{occ}	1.00	1.00
Reability factors		
χ^2	0.748	1.02
R_p (%)	4.83	4.81
R_{wp} (%)	5.90	6.16
R_{exp} (%)	7.16	6.29
R_B (%)	9.54	9.84

Table II contains the interatomic distances and angles after the Rietveld refinements of both oxidized and reduced samples at room temperature. The (Co,Ti-O1) bond-lengths at room temperature for the oxidized phase compare reasonably well with the expected value calculated as ionic radii sums, displaying values of 1.9931(4) Å *versus* the calculated 2.026 Å ($^{VI}Co^{2+}$: 0.650 Å; $^{VI}Ti^{4+}$: 0.605 Å) [15]. As expected, the <(Co,Ti)-O2> distances for the reduced sample (2.006 Å) increase as a consequence of the increase of the ionic size from Ti^{4+} (i.r.: 0.605 Å) to Ti^{3+} (i.r.: 0.650 Å).

Table II. Selected atomic distances (Å) and angles (deg) for the oxidized and reduced $LaM_{0.5}Ti_{0.5}O_3$ (M= Co and Ni) at 295 K.

M	**Co (oxid)**	**Co (red)**
Distances (Å)		
La – O1	2.932(2)	2.993(2)
	2.651(2)	2.617(2)
	3.158(3)	3.151(2)
	2.395(3)	2.422(2)
<La – O1>	**2.784**	**2.795**
Ti/M – O1 (x2)	1.9931(4)	1.9988(3)
Ti/M – O2 (x2)	1.946(1)	2.010(1)
(x2)	2.039(1)	1.993(1)
<Ti/M – O2>	**1.993**	**2.006**
Angles		
Ti/M – O1 – Ti/M	158.25(2)	158.59(2)
Ti/M – O2 – Ti/M	158.84(5)	157.04(3)

3.2 Thermal analysis (TGA)

The thermal evolution of the sample was studied by recording TGA curves. Heating $LaCo_{0.5}Ti_{0.5}O_3$ in $5\%H_2/95\%N_2$ atmosphere leads to the reduction of the sample to give $LaCo_{0.5}Ti_{0.5}O_{3-\delta}$ with the same crystal structure. The left panel of Fig 4 depicts the stability of the oxidized sample; in the right panel the auxotherm run is followed by an isotherm treatment at 600ºC required to stabilize the stoichiometry of the reduced sample, displaying the loss of 0.12 oxygen atoms at this temperature. The calculated value is in good agreement with the NPD data (Table I), leading to a $LaCo_{0.5}Ti_{0.5}O_{2.88}$ composition. The thermal analysis confirmed the existence of a mixed valence in the reduced phase. A thermal treatment of the resulting reduced phase in oxidizing (air) atmosphere restores the perovskite phase, thus confirming the required reversibility upon cycling in oxidizing-reducing atmospheres.

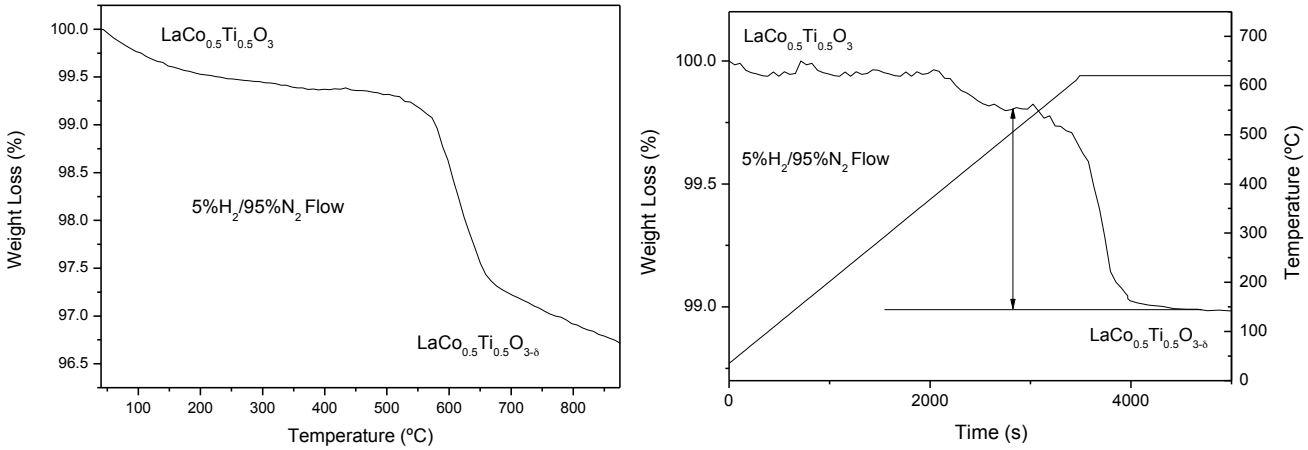

Fig. 4. Left panel: TG curve of $LaCo_{0.5}Ti_{0.5}O_3$ in reducing conditions; right panel: auxotherm run followed by an isotherm treatment at 600ºC where the reduced specimen is stabilized.

3.3. Thermal expansion measurements.

Aiming to determine the mechanical compatibility of our material with the other cell components, thermal expansion measurement of the dense ceramic was carried out in different atmospheres. The thermal expansion of the perovskite phases were measured in sintered pellets, initially heated in air at 900 ºC for 12 h; the reduced phase was finally treated in a 5% H_2 flow at 800 ºC for 4h. A dilatometric analysis was performed between 35 and 800 ºC for several cycles; the data where only recorded during the heating runs. Fig. 5 shows no abrupt changes in the thermal expansion of oxidized and reduced $LaCo_{0.5}Ti_{0.5}O_3$ in all the temperature range under measurement. The TEC measured in air atmosphere between 100 and 800 ºC is 10.43×10^{-6} K^{-1} for the oxidized phase. The thermal expansion of the reduced phase shows a value of 12.63×10^{-6} K^{-1} when heating the sample in $H_2(5\%)/N_2(95\%)$, very similar to that obtained for the oxidized perovskite. The determined TEC values match with those of other cell components and are certainly lower than those reported for some cobaltites, as expected by the partial substitution of Co by Ti.

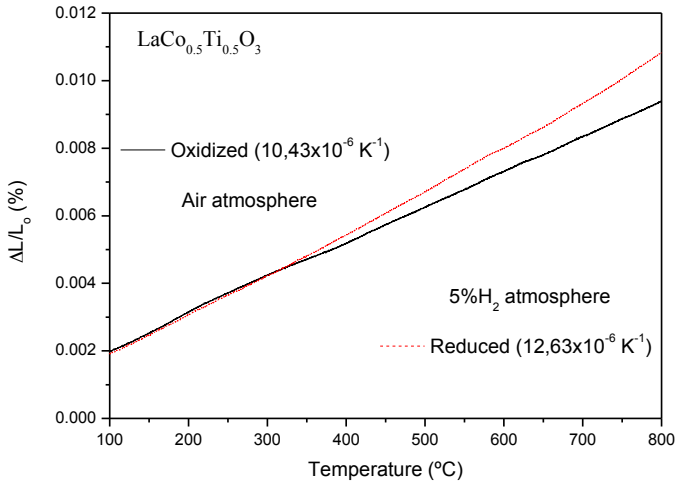

Fig.5. Thermal expansion determined by dilatometry for $LaM_{0.5}Ti_{0.5}O_3$ (oxidized and reduced).

3.4 Electrical conductivity measurements

Fig. 6 shows the thermal variation of the electrical conductivity of $LaCo_{0.5}Ti_{0.5}O_3$ measured twice, in order to be sure, in sintered bars in $5\%H_2/95\%N_2$ atmosphere by the *dc* four-probe method. The reduced phase shows a semiconductor-like behavior under reducing conditions with a maximum value of 0.27 $S{\cdot}cm^{-1}$ at 850 ºC. Although the conductivity values obtained are lower than 0.5 Scm^{-1}, it is not necessary such high values for the anode materials in single oxide fuel cells. Although the reduced $LaCo_{0.5}Ti_{0.5}O_{3-\delta}$ perovskite was prepared under a $5\%H_2/95\%N_2$ flow at 600 ºC, this phase is stable up to 750 ºC, as checked by TG measurements. Beyond this temperature there is a slight weight loss which suggests a partial reduction of the oxygen stoichiometry; this would correspond only to the last two conductivity points, and, indeed, both conductivity and thermal expansion curves show a monotonic behavior in all the temperature range

Fig. 6 also illustrates the electrical conductivity of the oxidized $LaCo_{0.5}Ti_{0.5}O_3$ perovskite, measured in an air atmosphere. The phase display also a semiconductor-like behavior, with conductivity values much lower than for the reduced sample with a maximum value of 0.07 Scm^{-1} at 900ºC. The reduced $LaCo_{0.5}Ti_{0.5}O_3$ perovskite, containing mixed Ti^{3+}-Ti^{4+} valence, presents a higher electrical conductivity by electron hopping between adjacent Ti^{3+} and Ti^{4+} cations (due to the antisite disordering), but the presence of M^{2+} ions hinders the long-range conduction path and promotes a low electronic conductivity.

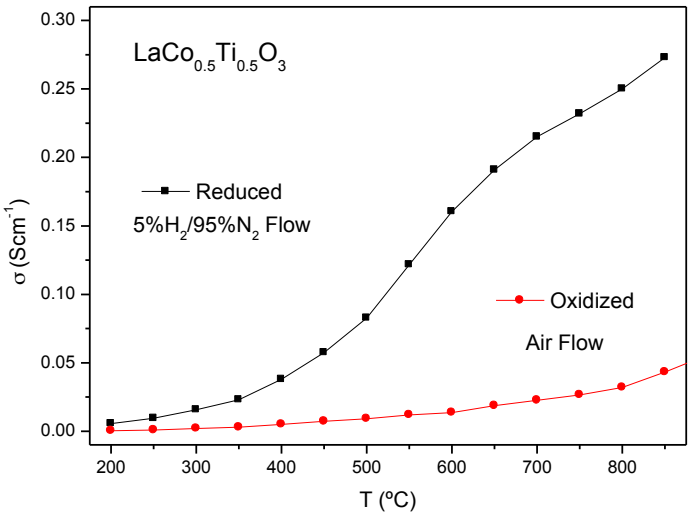

Fig.6. *dc*-conductivity as a function of temperature for $LaCo_{0.5}Ti_{0.5}O_3$ (oxidized and reduced).

4. Conclusions

In this work, we have prepared oxygen-stoichiometric $LaCo_{0.5}Ti_{0.5}O_3$ perovskite, containing Co^{2+} and Ti^{4+}, by soft chemistry procedures followed by thermal treatments in air. A topotactic reduction of the stoichiometric perovskites, in a reduced atmosphere, leads to oxygen-deficient phase with $LaCo_{0.5}Ti_{0.5}O_{2.91}$ compositions, where Ti^{4+} is partially reduced to Ti^{3+}, as shown by both neutron diffraction and thermogravimetric analysis. The expansion of the unit-cell volume ions in the reduced sample, the increase of the <Co,Ti-O> bond lengths and the localization of oxygen vacancies at the axial positions of the perovskite are sizeable proofs of the presence of Ti^{3+} cations in the specimen.

The crystal structure of both the oxidized and reduced $LaCo_{0.5}Ti_{0.5}O_3$ have been refined at RT in the orthorhombic *Pbnm* space group; the Co and Ti atoms are randomly distributed and no crystallographic long-range order was observed. The electrical characterization evidences a

semiconductor behavior in all the samples displaying a maximum value of 0.27 Scm^{-1} in the reduced specimen. The thermal expansion coefficients for the oxidized and reduced phases perfectly match with the standard values of SOFCs electrolytes. The reversibility of the reduction-oxidation of the $LaCo_{0.5}Ti_{0.5}O_3$ makes it possible the required cyclability of the cells.

Acknowledgments
We thank the financial support of the Spanish Ministry of Science and Innovation (MICINN) to the project MAT2010-16404; AA and DPC also wish to thank to MICINN for a "Juan de la Cierva" and a "Ramón y Cajal" contracts, respectively. We are grateful to the Institut Laue-Langevin (ILL) in Grenoble for making all facilities available.

References

[1] Mitchell RH 2002 *Perovskites, Modern and Ancient* (Almaz Press, Ontario)
[2] Aguadero A, Alonso JA, Martínez-Lope MJ, Fernández-Díaz MT 2011 *Solid State Sciences* **13** 13-18.
[3] Tokura Y, Taguchi T, Okada Y, Fujishima Y, Arima T, Kumagai K, Iye Y. 1993 *Phys. Rev. Lett.* **70 (14)** 2126–2129.
[4] Okaka Y, Arima T, Tokura Y, Murayama C, Mori N. 1993 *Phys. Rev. B* **48 (13)** 9677–9683.
[5] Robey SW, Hudson LT, Eylem C, Eichorn B. 1993 *Phys. Rev. B* **48 (1)** 562–568.
[6] Sunstrom JE, Kauzlarich SM. 1993 *Chem. Mater.* **5** 1539–1544.
[7] Kamegashira N, Nakajima N, Watanabe K, Kobayashi M. 2000 *Journal of Alloys and Comp.* **311** 74-78.
[8] Alvarez-Serrano I, Cuello GJ, Lopez ML, Jimenez-Lopez A, Pico C, Rodriguez-Castellon E, Rodriguez E, Veiga ML. 2008 *J. Phys. D: Appl. Phys.* **41** 195001.
[9] Holman KL, Huang Q, Klimczuk T, Trzebiatowski K, Bos JWG, Morosan E, Lynn JW, Cava JR. 2007 *Journal of Solid State Chemistry.* **180** 75–83.
[10] Rodríguez E, López ML, Campo J, Veiga ML, Pico C. 2002 *Journal of Materials Chemistry* **12 (9)** 2798-2802.
[11] Cairns DL, Reaney IM, Zheng H, Iddles D, Price T. 2005 *Journal of European Ceramic Society.* **25** 433-439.
[12] Ramadass N, Gopalakrishnan J, Sastri MVC 1978 *J. Inorg. Nucl. Chem.* **40** 1453–1454
[13] Rietveld HM 1969 *J. Appl. Crystallogr.* **2** 65-71.
[14] Rodríguez-Carvajal J 1993 *Physica B.* **192** 55-69.
[15] Shannon RD 1976 *Acta Crystallogr. A* **32** 751-767.